

## Simple model for sequential multiphoton ionization by ultraintense x rays

Xiang Li <sup>1,2</sup>, Rebecca Boll,<sup>3</sup> Daniel Rolles <sup>1</sup>, and Artem Rudenko<sup>1</sup>

<sup>1</sup>*J. R. Macdonald Laboratory, Department of Physics, Kansas State University, Manhattan, Kansas 66506, USA*

<sup>2</sup>*Linac Coherent Light Source, SLAC National Accelerator Laboratory, Menlo Park, California 94025, USA*

<sup>3</sup>*European XFEL, Holzkoppel 4, 22869 Schenefeld, Germany*



(Received 20 July 2021; accepted 9 September 2021; published 22 September 2021)

A simple model for sequential multiphoton ionization by ultraintense x rays is presented. The derived scaling of the ion yield with pulse energy quantitatively reproduces the experimental data, which shows that the ion yield increases according to the “power-law” behavior typical of multiphoton ionization, followed by saturation at high pulse energies. The calculated average time interval between ionizations for producing ions at a certain charge state is found to be proportional to the pulse duration and independent of all other x-ray pulse parameters. This agrees with previous studies where the kinetic energy of fragment ions with a given charge state produced by the intense x-ray ionization of molecules was found to be independent of the pulse energy, but to increase with a smaller pulse duration due to the smaller time interval between ionizations.

DOI: [10.1103/PhysRevA.104.033115](https://doi.org/10.1103/PhysRevA.104.033115)

### I. INTRODUCTION

At photon energies smaller than 100 keV, photoabsorption and scattering are the two major processes underlying the interaction of x rays with matter, with photoabsorption being several orders of magnitude more probable than scattering at photon energies below 10 keV. In an ultraintense pulse generated by an x-ray free-electron laser (XFEL), which typically contains  $\sim 10^{12}$  photons within a pulse duration of a few tens of femtoseconds, multiple x-ray photons can be absorbed by an atom [1,2] or a molecule [3], generating extremely high-charged ionic states [4,5]. If the x-ray photon energy is high enough, the process usually occurs sequentially, and each of the absorption events leads to ionization, as confirmed by many experimental studies of the interaction of XFEL pulses with atoms [2,4,6] and molecules [3,5,7–10]. Such sequential multiphoton ionization is also the source of radiation damage in coherent imaging experiments with XFELs [11–14]. Theoretically, the interaction of ultraintense x rays with atoms and molecules, driven by the sequential multiphoton ionization process, has mostly been treated with *ab initio* approaches based on “rate-equation” [2,15] and Monte Carlo methods [16–19], and good agreement with the experimental results has been achieved [2,4–6,20].

In this paper, we introduce a simple model to describe the sequential multiphoton ionization process. The scaling of ion yields with pulse energy and the average time interval between ionizations are derived without the need to implement computationally intensive *ab initio* calculations. By assuming the XFEL pulse to have a Gaussian temporal profile, the number of photoabsorptions to be  $n$ , and the photoabsorption cross section for each ionization step to be  $\sigma$ , the differential probability for  $n$  photoabsorption events to occur at times  $t_1, t_2, \dots, t_n$  is derived. Based on this probability, we obtain the functional dependence of the probability for sequential

$n$ -photon ionization to occur, as well as the average timing for each of these  $n$  ionization steps. The functional dependence of the sequential  $n$ -photon ionization probability is then used to calculate the scaling of the ion yield with pulse energy. It is found to quantitatively describe the behavior of the measured ion yields showing a “power-law” increase followed by saturation, as was also observed in previous FEL experiments [1,4,21–23]. The average time interval between ionizations for producing a given charge state is found to depend only on the pulse duration with a proportional relation, and not on any other pulse parameters, which is consistent with the conclusion drawn from a previous experiment studying the ultraintense hard x-ray ionization of  $\text{CH}_3\text{I}$  molecules [24]. In that experiment, the kinetic energy of iodine ion fragments was found to be independent of pulse energy, and to increase with shorter pulse durations because of the decreased time interval between ionizations. In addition to providing general insight on the process of sequential multiphoton ionization, the model can be used to simulate the charge buildup process leading to the explosion of molecules, which is relevant, e.g., for Coulomb explosion imaging at XFEL facilities.

### II. SEQUENTIAL MULTIPHOTON IONIZATION MODEL

For the simplest case of two-photon ionization, the differential probability for the two photons being absorbed with a time interval  $\Delta t$  was derived in Ref. [25]. This differential probability was then used to calculate the probability distribution of the kinetic energy release of the ionized molecules. Here, we study the general case where the interaction involves the sequential absorption of an arbitrary number of photons. Specifically, we consider an arbitrary final interaction product requiring a sequence of  $n$  photoabsorptions from a Gaussian XFEL pulse with a photon flux  $F(t) = f e^{-4 \ln 2 (\frac{t}{\tau})^2}$ , where  $f$

is the peak photon flux and  $\tau$  is the pulse duration (full width at half maximum).

Assuming a uniform photoabsorption cross section  $\sigma$  for each ionization step, the differential probability for the sequence of  $n$  ionizations to occur at times  $t_1, t_2, \dots$ , and  $t_n$  is

$$\begin{aligned} \frac{dP}{dt_1 dt_2 \cdots dt_n} &= e^{-\int_{-\infty}^{t_1} F(t)\sigma dt} F(t_1)\sigma e^{-\int_{t_1}^{t_2} F(t)\sigma dt} F(t_2)\sigma \cdots e^{-\int_{t_{n-1}}^{t_n} F(t)\sigma dt} F(t_n)\sigma e^{-\int_{t_n}^{\infty} F(t)\sigma dt} \\ &= \sigma^n F(t_1)F(t_2) \cdots F(t_n) e^{-\int_{-\infty}^{\infty} F(t)\sigma dt} \\ &= e^{-\sqrt{\frac{\pi}{4\ln 2}}\sigma\tau f} \sigma^n F(t_1)F(t_2) \cdots F(t_n). \end{aligned} \quad (1)$$

The differential probability for the sequence of  $n$  ionizations to occur at time intervals  $\Delta t_{2,1}, \Delta t_{3,1}, \dots, \Delta t_{n,1}$  [with  $\Delta t_{n,1} = (t_n - t_1)$ ,  $i = 2, 3, \dots, n$ ] is

$$\begin{aligned} \frac{dP}{d\Delta t_{2,1} d\Delta t_{3,1} \cdots d\Delta t_{n,1}} &= \int_{-\infty}^{\infty} \int_{t_1}^{\infty} \cdots \int_{t_{n-1}}^{\infty} \frac{dP}{dt_1 dt_2 \cdots dt_n} \delta[\Delta t_{2,1} - (t_2 - t_1)] \\ &\quad \times \delta[\Delta t_{3,2} - (t_3 - t_2)] \cdots \delta[\Delta t_{n,n-1} - (t_n - t_{n-1})] dt_n \cdots dt_2 dt_1 \\ &= e^{-\sqrt{\frac{\pi}{4\ln 2}}\sigma\tau f} \sigma^n \int_{-\infty}^{\infty} \int_{t_1}^{\infty} \cdots \int_{t_{n-1}}^{\infty} F(t_1) \delta[\Delta t_{2,1} - (t_2 - t_1)] F(t_2) \delta[\Delta t_{3,2} - (t_3 - t_2)] \cdots \\ &\quad \times F(t_{n-1}) \delta[\Delta t_{n,n-1} - (t_n - t_{n-1})] F(t_n) dt_n \cdots dt_2 dt_1 \\ &= e^{-\sqrt{\frac{\pi}{4\ln 2}}\sigma\tau f} \sigma^n f^n \int_{-\infty}^{\infty} e^{[-\frac{4\ln 2}{\tau^2}(t_1^2 + (t_1 + \Delta t_{2,1})^2 + \cdots + [t_1 + (\Delta t_{2,1} + \Delta t_{3,2} + \cdots + \Delta t_{n,n-1})]^2)]} dt_1 \\ &= e^{-\sqrt{\frac{\pi}{4\ln 2}}\sigma\tau f} \sigma^n f^n e^{4\ln 2 \frac{A^2 - nB}{n\tau^2}}, \end{aligned} \quad (2)$$

where  $A = \Delta t_{2,1} + \Delta t_{3,1} + \cdots + \Delta t_{n,1}$  and  $B = \Delta t_{2,1}^2 + \Delta t_{3,1}^2 + \cdots + \Delta t_{n,1}^2$ , with  $\Delta t_{2,1} \leq \Delta t_{3,1} \leq \cdots \leq \Delta t_{n,1}$ .

The assumption of a uniform cross-section value over different ionization steps is made for two reasons. One is that the (deep) inner-shell photoabsorption cross section for a given molecule typically does not depend strongly on the charge state, provided that the photon energy is far above the ionization threshold of the nearest subshell, no transient resonance occurs, and higher-order effects such as x-ray induced transparency are negligible. Although there are certainly many examples where this assumption would not be justified, this condition can often be fulfilled for XFEL pulses. Another reason is that it allows us to obtain the sequential ionization probabilities and the distribution of ionization time intervals as closed-form expressions, which is beneficial for the comparison with the experimental data. This assumption leaves some flexibility in how the cross-section value is chosen. We would expect that taking  $\sigma$  as the average of the cross-section values over different ionization steps (as opposed to the cross-section value for the first ionization step) gives a more accurate result for the probability of sequential ionizations to be discussed in Secs. II A and III A, as well as for the average time interval between adjacent ionizations to be discussed in Secs. II B and III B.

#### A. Probability for sequential $n$ -photon ionization and scaling of the ion yield with pulse energy

By integrating Eq. (2) over all possible time intervals, the probability  $P_n$  to get to a certain interaction product requiring  $n$ -photon absorption can be obtained,

$$P_n = a e^{-bf} f^n, \quad (3)$$

where  $a$  is a constant depending on the photon number  $n$  and pulse duration  $\tau$ , and  $b = \sqrt{\frac{\pi}{4\ln 2}}\sigma\tau$ . It is worth noting that Eq. (3) takes a similar form as Eq. (6) in Ref. [21], which is derived by analytically solving the rate equations. There are three major differences between the present model and the one in Ref. [21]. One is that the current model starts with the differential probability for the sequence of  $n$  ionizations to occur at times  $t_1, t_2, \dots, t_i, \dots$ , and  $t_n$ . It is expressed in Eq. (2) as a sequence of multiplications of the probabilities for each of the ionizations to happen at a particular time and not at other times. In contrast, the model in Ref. [21] starts with a set of rate equations with each rate equation describing the change of each charge state due to transitions to or from other charge states. The second difference is that the time  $t_i$  at which the  $i$ th photoionization occurs, as well as the time intervals  $t_{i1}$  between the  $i$ th ionization and the first, is explicitly introduced in the present model, which is necessary for the discussion of the average time interval of the  $n$  sequential ionizations in Sec. II B. The third difference is that for the derivation of Eq. (3), we assumed the x-ray pulse (with duration  $\tau$  and peak flux  $f$ ) to be a Gaussian function  $F(t) = f e^{-4\ln 2 (\frac{t}{\tau})^2}$ . In contrast, the derivation in Ref. [21] used an effective pulse duration  $\tau_\infty$ , which was calculated by  $\tau_\infty = \int_{-\infty}^{\infty} f(t') dt'$  with  $f(t')$  being the dimensionless temporal shape of the x-ray pulse.

Equation (3) can be rewritten in terms of the per-shot ion yield  $Y_n$  (which is related to  $P_n$  by  $Y_n = NP_n$ , with  $N$  being the number of target atoms or molecules in the interaction volume) and pulse energy  $E_{\text{pls}}$  (which is the quantity measured in the experiment, and can be approximately related to the photon flux  $f$  by  $E_{\text{pls}} = \frac{\tau A E_{\text{pho}}}{c_l} f$ , with  $E_{\text{pho}}$  being the photon energy,  $A$  being the effective x-ray focal area, and  $c_l$  the

beamline transmission coefficient),

$$Y_n = c e^{-dE_{\text{pls}}} E_{\text{pls}}^n, \quad (4)$$

where  $c$  is the constant depending on  $n$ ,  $\tau$ ,  $N$ ,  $c_t$ , and  $A$ , and  $d = \frac{\sqrt{\frac{\pi}{4 \ln 2}} \sigma c_t}{A E_{\text{pho}}}$ .

### B. Average time interval of the $n$ sequential ionizations

We normalize  $\frac{dP}{d\Delta t_{2,1} d\Delta t_{3,1} \dots d\Delta t_{n,1}}$  in Eq. (2) such that

$$\begin{aligned} & \int_0^\infty \int_0^{\Delta t_{n,1}} \dots \int_0^{\Delta t_{3,1}} G_n \frac{dP}{d\Delta t_{2,1} d\Delta t_{3,1} \dots d\Delta t_{n,1}} \\ & \times d\Delta t_{2,1} \dots d\Delta t_{n-1,1} d\Delta t_{n,1} \\ & = \int_0^\infty \int_0^{\Delta t_{n,1}} \dots \int_0^{\Delta t_{3,1}} C_n e^{4 \ln 2 \frac{A^2 - nB}{n\tau^2}} \\ & \times d\Delta t_{2,1} \dots d\Delta t_{n-1,1} d\Delta t_{n,1} \\ & = 1, \end{aligned} \quad (5)$$

with  $G_n$  and  $C_n$  being the normalization constants. Note that the total ionization probability equals  $\frac{1}{G_n}$  is assumed for this normalization. Based on Eq. (5), the probability distribution  $D_n(\Delta t_{2,1}, \Delta t_{3,1}, \dots, \Delta t_{n,1})$  of the time interval sequence  $\Delta t_{2,1}, \Delta t_{3,1}, \dots, \Delta t_{n,1}$  can be obtained as

$$D_n(\Delta t_{2,1}, \Delta t_{3,1}, \dots, \Delta t_{n,1}) = C_n e^{4 \ln 2 \frac{A^2 - nB}{n\tau^2}}. \quad (6)$$

In Eqs. (5) and (6),  $C_n$  does not depend on the peak intensity  $f$  and the cross section  $\sigma$  because they are only in the constant  $e^{-\sqrt{\frac{\pi}{4 \ln 2}} \sigma \tau f} \sigma^n f^n$  of the unnormalized Eq. (2) and are canceled out with the normalization procedure. So the probability distribution  $D_n(\Delta t_{2,1}, \Delta t_{3,1}, \dots, \Delta t_{n,1})$  in Eq. (6) only depends on the pulse duration  $\tau$ , which makes that the average time interval between ionizations to be derived from this probability distribution only depends on the pulse duration as well. The sequential  $n$ -photon ionization therefore becomes more likely with a larger peak photon flux as shown by Eq. (3), but the average time interval between ionizations stays the same as long as the pulse duration is not changed.

In the following, Eq. (6) will be applied to the specific cases of sequential two- and three-photon ionizations. For sequential two-photon ionizations, the probability distribution for the time interval  $\Delta t_{2,1}$  is

$$D_2(\Delta t_{2,1}) = C_2 e^{-2 \ln 2 \frac{\Delta t_{2,1}^2}{\tau^2}}, \quad (7)$$

with the normalization constant  $C_2 = \frac{2\sqrt{2 \ln 2}}{\sqrt{\pi} \tau}$ . From Eq. (7), the average time interval between the two photoionizations is

$$\begin{aligned} \overline{\Delta t_{2,1}} &= \int_0^\infty \Delta t_{2,1} D_2(\Delta t_{2,1}) d\Delta t_{2,1} \\ &= \frac{\tau}{\sqrt{2\pi \ln 2}}. \end{aligned} \quad (8)$$

For example, if a certain interaction product is created by two photoionizations within a 30-fs XFEL pulse, the average time interval is  $\overline{\Delta t_{2,1}} = \frac{1}{\sqrt{2\pi \ln 2}} \times 30 \text{ fs} \approx 14 \text{ fs}$ .

For three sequential photoionizations, the probability distribution for the time intervals  $\Delta t_{2,1}$  and  $\Delta t_{3,1}$  is

$$D_3(\Delta t_{2,1}, \Delta t_{3,1}) = C_3 e^{-4 \ln 2 \frac{-2\Delta t_{2,1}^2 + 2\Delta t_{2,1}\Delta t_{3,1} - 2\Delta t_{3,1}^2}{3\tau^2}}, \quad (9)$$

with the normalization constant  $C_3 = \frac{48 \ln 2}{\sqrt{3\pi} \tau^2}$ . From Eq. (9), the average time interval between the first and last photoionizations can be calculated:

$$\begin{aligned} \overline{\Delta t_{3,1}} &= \int_0^\infty \int_0^{\Delta t_{3,1}} \Delta t_{3,1} D_3(\Delta t_{2,1}, \Delta t_{3,1}) d\Delta t_{2,1} d\Delta t_{3,1} \\ &= \frac{3}{2\sqrt{2\pi \ln 2}} \tau. \end{aligned} \quad (10)$$

If a certain interaction product is created by three photoionizations within a 30-fs XFEL pulse, the average time interval is thus  $\overline{\Delta t_{3,1}} = \frac{3}{2\sqrt{2\pi \ln 2}} \times 30 \text{ fs} \approx 22 \text{ fs}$ .

The average time intervals for interactions with larger numbers of sequential photoionizations can be calculated analogously as for the sequential three-photon ionization. For the general case of sequential  $n$ -photon ionization, it is shown in the following that the average time interval is proportional to the pulse duration  $\tau$ .

Introducing the scaled time interval  $\Delta t'_{i,1} = \frac{\Delta t_{i,1}}{\tau}$ , with  $i = 2, 3, \dots, n$ , the distribution for these scaled time intervals is

$$D'_n(\Delta t'_{2,1}, \Delta t'_{3,1}, \dots, \Delta t'_{n,1}) = C'_n e^{4 \ln 2 \frac{A'^2 - nB'}{n}}, \quad (11)$$

where  $C'_n$  is the normalization constant, which does not depend on  $\tau$ ,  $A' = \Delta t'_{2,1} + \Delta t'_{3,1} + \dots + \Delta t'_{n,1}$ , and  $B' = \Delta t'^2_{2,1} + \Delta t'^2_{3,1} + \dots + \Delta t'^2_{n,1}$ , with  $\Delta t'_{2,1} \leq \Delta t'_{3,1} \leq \dots \leq \Delta t'_{n,1}$ . Since  $D'_n(\Delta t'_{2,1}, \Delta t'_{3,1}, \dots, \Delta t'_{n,1})$  does not depend on  $\tau$ , neither does the average time interval  $\overline{\Delta t'_{n,1}}$ , which can be obtained from

$$\begin{aligned} \overline{\Delta t'_{n,1}} &= \int_0^\infty \int_0^{\Delta t'_{n,1}} \dots \int_0^{\Delta t'_{3,1}} \Delta t'_{n,1} D'_n(\Delta t'_{2,1}, \Delta t'_{3,1}, \dots, \Delta t'_{n,1}) \\ & \times d\Delta t'_{2,1} \dots d\Delta t'_{n-1,1} d\Delta t'_{n,1}. \end{aligned} \quad (12)$$

The unscaled average time interval is then  $\overline{\Delta t_{n,1}} = \overline{\Delta t'_{i,1}} \tau \propto \tau$ .

## III. APPLICATION OF THE SIMPLE MODEL

### A. Scaling of the ion yield with pulse energy

Equation (4) can be used to describe the dependence of the ion yield on the x-ray pulse energy. In Fig. 1, the experimental ion yield per shot for three representative ions,  $\text{I}^{2+}$ ,  $\text{I}^{15+}$ , and  $\text{I}^{26+}$ , created by the interaction between  $\text{CH}_3\text{I}$  molecules and 2-keV x rays generated by the European X-ray Free-Electron Laser, are plotted as a function of pulse energy as measured upstream of the Small Quantum Systems (SQS) instrument, together with the fits by using the function in Eq. (4).

The parameters  $c$  and  $d$ , which are dependent on experimental settings (such as the beam focal area) are used as fitting parameters since they cannot be easily predetermined. The average number of photoabsorptions  $n$  can be preestimated by energy arguments. One photoabsorption is enough to reach  $\text{I}^{2+}$ , thus  $n$  was set to 1 to fit the  $\text{I}^{2+}$  ion yield. The minimum number of photoabsorptions required to reach the other two charge states can be estimated by applying energy

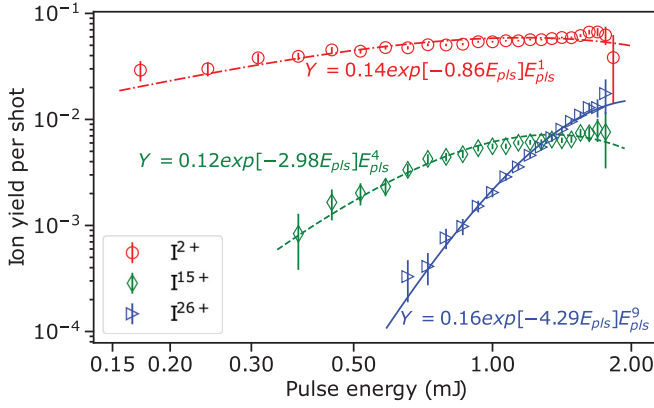


FIG. 1. Yield of  $I^{2+}$ ,  $I^{15+}$ , and  $I^{26+}$  as a function of pulse energy, produced by the interaction between  $\text{CH}_3\text{I}$  molecules and 2-keV x rays generated by the European X-ray Free-Electron Laser. The pulse energy was measured upstream of the Small Quantum Systems instrument, in which the experiment was performed. These data are “noncoincident,” i.e., integrated over all carbon ion charge states. The experimental data are shown by circles, diamonds, and triangles for  $I^{2+}$ ,  $I^{15+}$ , and  $I^{26+}$ , respectively. The dotted-dashed, dashed, and solid lines are the corresponding fits using Eq. (4), with the fitted functions displayed in the figure.

conservation. We take the production of  $I^{26+}$  as an example. The total energy of electrons in the neutral  $\text{CH}_3\text{I}$  molecule is approximately the sum of the energy of the electrons in the individual atoms, which is  $-198.369$  keV. When  $I^{26+}$  is produced, its coincident carbon partner most likely has four charges, and all three hydrogen fragments are also charged, as shown in Figs. 5.1 and 6.2 of Ref. [26]. The total energy of electrons in the fragments ( $I^{26+}$ ,  $\text{C}^{4+}$ ,  $3 \times \text{H}^+$ ) is  $-187.646$  keV. The average energy of photoelectrons ionized for the production of  $I^{26+}$  is  $0.599$  keV. (These energy calculations were made with the Hartree-Fock method through Cowan’s atomic code [27,28].) From energy conservation, the total energy of absorbed photons subtracted by the total energy of photoelectrons, which is  $(n \times 2 - n \times 0.599)$  keV, should be equal to or larger (to account for radiative decay processes) than the energy change in the molecular system, which is  $(198.369 - 187.646)$  keV. The minimum of  $n$  satisfying this requirement is 8. So,  $n = 9$  is used, in order to also account for possible radiative decays and the fact that the total energy of the neutral molecule is smaller than that estimated with the independent-atom model. (A more precise estimate of the number of photons needed to reach a particular charge state requires a detailed knowledge of the average decay pathways involved.) With  $n$  thus determined to be 1, 4, and 9 for  $I^{2+}$ ,  $I^{15+}$ , and  $I^{26+}$ , respectively, Eq. (4) is used to fit the experimental data. The resulting function for each charge state is displayed in Fig. 1. The fitting values for  $d$  contain information about the x-ray transmission, focal area, and photoabsorption cross section. For x rays with a photon energy of 2 keV, the photoabsorption cross section  $\sigma$  for the  $\text{CH}_3\text{I}$  molecule is approximately that of iodine, which is  $0.4$  Mb [29]. Using this value for  $\sigma$ , a typical beamline transmission coefficient  $c_t$  of  $0.8$ , and the fitting values of  $d$  for  $I^{2+}$ ,  $I^{15+}$ , and  $I^{26+}$ , the calculated effective focal areas are about 124,

36, and  $25 \mu\text{m}^2$ , respectively. These values are larger than the expected focal area  $\sim 1 \mu\text{m}^2$ , because with the applied formula  $E_{\text{pl}s} = \frac{\tau A E_{\text{pho}}}{c_t} f$ , the effective focal area  $A$  is the average beam area in the whole interaction region, which is much larger than the focal area at the beam center. The observation that higher-charged ions have smaller effective focal areas can be attributed to the fact that such ions require a higher x-ray intensity and hence are produced in a more confined region around the x-ray focus. If the beamline transmission and effective focal area are known, the fitting value for  $d$  can also be used to calculate the (average) photoabsorption cross section. It is worth noting that such calculations of the effective focal area  $A$  and average cross section assume that the average number  $n$  of photoabsorptions is known beforehand. For more precise calculations, a more accurate method to estimate  $n$  is required. In addition, if the parameter  $d$  can be determined by independent measurements, the number of photoabsorptions  $n$  and the parameter  $c$  can be used as fitting parameters, providing a way to measure the average number of photoabsorptions required to reach a certain interaction product.

According to Eq. (4), the yield of a particular charge state requiring  $n$  photoabsorptions initially follows a power law, i.e.,  $Y_n \propto E_{\text{pl}s}^n$ , in the low pulse energy range. At higher pulse energies, the exponential factor  $e^{-d E_{\text{pl}s}}$  becomes non-negligible, and the ion yield starts to saturate and eventually decreases with increasing pulse energy. This describes the fact that if the pulse energy continues to increase, only the highest energetically achievable charge state, which cannot be further ionized, is left as the final interaction product, while all other ion charge states are depleted.

## B. Average time interval of the $n$ sequential ionizations

Since the probability for a single photoionization increases with the photon flux or pulse intensity, it is tempting to conclude that the average time interval of the  $n$  sequential ionizations decreases with these two quantities. However, within the sequential multiphoton ionization model introduced in Sec. II B, the time interval is proportional to the pulse duration  $\tau$  and independent of all other pulse parameters such as photon flux.

The average time interval between ionizations cannot be easily studied with experiments using atomic targets. For molecular targets, however, it is reflected in the fragment ion kinetic energies. If the time interval is small, the ion kinetic energy would be large because with ionizations separated by small time intervals, a certain ion charge state is reached at a short internuclear distance, which causes stronger Coulomb repulsion. The dependence of the average time interval between ionizations on the x-ray pulse parameters can therefore be studied by measuring the kinetic energy of ions produced from the ionization of molecules by x rays with different pulse energies or durations. In a previous study [24], where we investigated the pulse energy and pulse duration dependence of the ultraintense hard x-ray ionization of  $\text{CH}_3\text{I}$  molecules, the iodine ion kinetic energy was found to be independent of pulse energy, but increased with a shorter pulse duration. This experimental observation supports the conclusion reached from the sequential multiphoton ionization model that the average

time interval between ionizations is proportional to the pulse duration  $\tau$  and independent of all other pulse parameters. An intuitive picture which explains such a pulse parameter dependence can be found in Ref. [24].

As an example of how the sequential model can be used in practice, we briefly discuss in the following how it can be applied to facilitate the interpretation of Coulomb explosion imaging experiments at XFEL facilities. To implement the Coulomb explosion imaging technique, Coulomb explosion simulations are required to compare with experimental observations. If the molecule is assumed to be instantaneously charged up, there will be a mismatch between the simulation and experimental observation due to the neglected charge buildup and redistribution processes [26,30]. To make a more accurate comparison possible, these two processes need to be included and the sequential multiphoton ionization model can be used to help simulate the charge buildup process. In particular, the experimental parameters such as the average number of photons required to reach a certain fragmentation product can be estimated by fitting the experimental data with Eq. (4), and the corresponding time interval between sequential photoionizations can be calculated according to the discussion in Sec. II B. These numbers can then be incorporated for simulating the charge buildup process.

#### IV. SUMMARY

A simple sequential multiphoton ionization model is presented, from which the probability for sequential  $n$ -photon ionization, the scaling of the ion yield with pulse energy, as well as the average time interval between ionizations can be calculated. The derived scaling of the ion yield with pulse energy in Eq. (4) contains a term describing the increase of the ion yield  $Y_n$  with pulse energy  $E_{\text{pls}}$  according to the power law  $Y_n \propto E_{\text{pls}}^n$ , as expected from a typical

$n$ -photon-absorption nonlinear process, and an exponentially decaying factor that describes saturation and depletion. The exponential factor can be neglected at small pulse energies but dominates the behavior at large pulse energies. Equation (4) is shown to quantitatively describe the “power-law”-type increase followed by saturation observed in the experimental data. The average time interval between ionizations calculated within the model is found to be proportional to the pulse duration and independent of all other pulse parameters. This is consistent with our previous experimental observation that the kinetic energy of fragment ions produced by the ionization of molecules with intense XFEL pulses is independent of pulse energy but increases with a smaller pulse duration due to the smaller time interval between ionizations.

Data recorded for the experiment at the European XFEL are available online [31].

#### ACKNOWLEDGMENTS

This work was funded by the US Department of Energy, Office of Science, Basic Energy Sciences (BES), Division of Chemical Sciences, Geosciences, and Biosciences, under Grants No. DE-FG02-86ER13491 (D.R. and A.R.) and DE-SC0019451 (X.L.). We thank the colleagues from the European XFEL and University of Frankfurt, who participated in the beamtime at the European XFEL, during which the experimental data shown in Fig. 1 were collected, which is used to demonstrate the application of our model. We also thank the scientific and technical staff of the European XFEL for their help and hospitality during the beamtime. We acknowledge valuable discussions with Ludger Inhester, Sang-Kil Son, and Robin Santra from the Center for Free-Electron Laser Science at DESY.

- 
- [1] A. A. Sorokin, S. V. Bobashev, T. Feigl, K. Tiedtke, H. Wabnitz, and M. Richter, Photoelectric Effect at Ultrahigh Intensities, *Phys. Rev. Lett.* **99**, 213002 (2007).
- [2] L. Young, E. P. Kanter, B. Krässig, Y. Li, A. M. March, S. T. Pratt, R. Santra, S. H. Southworth, N. Rohringer, L. F. DiMauro, G. Doumy, C. A. Roedig, N. Berrah, L. Fang, M. Hoener, P. H. Bucksbaum, J. P. Cryan, S. Ghimire, J. M. Glowia, D. A. Reis *et al.*, Femtosecond electronic response of atoms to ultra-intense X-rays, *Nature (London)* **466**, 56 (2010).
- [3] M. Hoener, L. Fang, O. Kornilov, O. Gessner, S. T. Pratt, M. Gühr, E. P. Kanter, C. Blaga, C. Bostedt, J. D. Bozek, P. H. Bucksbaum, C. Buth, M. Chen, R. Coffee, J. Cryan, L. DiMauro, M. Glowia, E. Hosler, E. Kuk, S. R. Leone *et al.*, Ultraintense X-Ray Induced Ionization, Dissociation, and Frustrated Absorption in Molecular Nitrogen, *Phys. Rev. Lett.* **104**, 253002 (2010).
- [4] B. Rudek, S.-K. Son, L. Foucar, S. W. Epp, B. Erk, R. Hartmann, M. Adolph, R. Andritschke, A. Aquila, N. Berrah, C. Bostedt, J. Bozek, N. Coppola, F. Filsinger, H. Gorke, T. Gorkhover, H. Graafsma, L. Gumprecht, A. Hartmann, G. Hauser *et al.*, Ultra-efficient ionization of heavy atoms by intense X-ray free-electron laser pulses, *Nat. Photonics* **6**, 858 (2012).
- [5] A. Rudenko, L. Inhester, K. Hanasaki, X. Li, S. J. Robatjazi, B. Erk, R. Boll, K. Toyota, Y. Hao, O. Vendrell, C. Bomme, E. Savelyev, B. Rudek, L. Foucar, S. H. Southworth, C. S. Lehmann, B. Kraessig, T. Marchenko, M. Simon, K. Ueda *et al.*, Femtosecond response of polyatomic molecules to ultra-intense hard X-rays, *Nature (London)* **546**, 129 (2017).
- [6] H. Fukuzawa, S.-K. Son, K. Motomura, S. Mondal, K. Nagaya, S. Wada, X.-J. Liu, R. Feifel, T. Tachibana, Y. Ito, M. Kimura, T. Sakai, K. Matsunami, H. Hayashita, J. Kajikawa, P. Johnsson, M. Siano, E. Kuk, B. Rudek, B. Erk *et al.*, Deep Inner-Shell Multiphoton Ionization by Intense X-Ray Free-Electron Laser Pulses, *Phys. Rev. Lett.* **110**, 173005 (2013).
- [7] B. Erk, D. Rolles, L. Foucar, B. Rudek, S. W. Epp, M. Cryle, C. Bostedt, S. Schorb, J. Bozek, A. Rouzee, A. Hundertmark, T. Marchenko, M. Simon, F. Filsinger, L. Christensen, S. De, S. Trippel, J. Küpper, H. Stapelfeldt, S. Wada *et al.*, Ultrafast Charge Rearrangement and Nuclear Dynamics upon Inner-Shell Multiple Ionization of Small Polyatomic Molecules, *Phys. Rev. Lett.* **110**, 053003 (2013).

- [8] B. Erk, R. Boll, S. Trippel, D. Anielski, L. Foucar, B. Rudek, S. W. Epp, R. Coffee, S. Carron, S. Schorb, K. R. Ferguson, M. Swiggers, J. D. Bozek, M. Simon, T. Marchenko, J. Kupper, I. Schlichting, J. Ullrich, C. Bostedt, D. Rolles *et al.*, Imaging charge transfer in iodomethane upon x-ray photoabsorption, *Science* **345**, 288 (2014).
- [9] K. Motomura, E. Kukk, H. Fukuzawa, S.-I. Wada, K. Nagaya, S. Ohmura, S. Mondal, T. Tachibana, Y. Ito, R. Koga, T. Sakai, K. Matsunami, A. Rudenko, C. Nicolas, X.-J. Liu, C. Miron, Y. Zhang, Y. Jiang, J. Chen, M. Anand *et al.*, Charge and nuclear dynamics induced by deep inner-shell multiphoton ionization of CH<sub>3</sub>I molecules by intense X-ray free-electron laser pulses, *J. Phys. Chem. Lett.* **6**, 2944 (2015).
- [10] K. Nagaya, K. Motomura, E. Kukk, H. Fukuzawa, S. Wada, T. Tachibana, Y. Ito, S. Mondal, T. Sakai, K. Matsunami, R. Koga, S. Ohmura, Y. Takahashi, M. Kanno, A. Rudenko, C. Nicolas, X.-J. Liu, Y. Zhang, J. Chen, M. Anand *et al.*, Ultrafast Dynamics of a Nucleobase Analogue Illuminated by a Short Intense X-ray Free Electron Laser Pulse, *Phys. Rev. X* **6**, 021035 (2016).
- [11] R. Neutze, R. Wouts, D. v. d. Spoel, E. Weckert, and J. Hajdu, Potential for biomolecular imaging with femtosecond X-ray pulses, *Nature (London)* **406**, 752 (2000).
- [12] A. Barty, S. Boutet, M. J. Bogan, S. Hau-Riege, S. Marchesini, K. Sokolowski-Tinten, N. Stojanovic, R. Tobey, H. Ehrke, A. Cavalleri, S. Düsterer, M. Frank, S. Bajt, B. W. Woods, M. M. Seibert, J. Hajdu, R. Treusch, and H. N. Chapman, Ultrafast single-shot diffraction imaging of nanoscale dynamics, *Nat. Photonics* **2**, 415 (2008).
- [13] K. Nass, L. Foucar, T. R. M. Barends, E. Hartmann, S. Botha, R. L. Shoeman, R. B. Doak, R. Alonso-Mori, A. Aquila, S. Bajt, A. Barty, R. Bean, K. R. Beyerlein, M. Bublitz, N. Drachmann, J. Gregersen, H. O. Jönsson, W. Kabsch, S. Kassemeyer, J. E. Koglin *et al.*, Indications of radiation damage in ferredoxin microcrystals using high-intensity X-FEL beams, *J. Synchrotron Radiat.* **22**, 225 (2015).
- [14] L. Galli, S.-K. Son, M. Klinge, S. Bajt, A. Barty, R. Bean, C. Betzel, K. R. Beyerlein, C. Caleman, R. B. Doak, M. Duszynski, H. Fleckenstein, C. Gati, B. Hunt, R. A. Kirian, M. Liang, M. H. Nanao, K. Nass, D. Oberthür, L. Redecke *et al.*, Electronic damage in S atoms in a native protein crystal induced by an intense X-ray free-electron laser pulse, *Struct. Dyn.* **2**, 041707 (2015).
- [15] N. Rohringer and R. Santra, X-ray nonlinear optical processes using a self-amplified spontaneous emission free-electron laser, *Phys. Rev. A* **76**, 033416 (2007).
- [16] S.-K. Son and R. Santra, Monte Carlo calculation of ion, electron, and photon spectra of xenon atoms in x-ray free-electron laser pulses, *Phys. Rev. A* **85**, 063415 (2012).
- [17] P. J. Ho, C. Bostedt, S. Schorb, and L. Young, Theoretical Tracking of Resonance-Enhanced Multiple Ionization Pathways in X-ray Free-Electron Laser Pulses, *Phys. Rev. Lett.* **113**, 253001 (2014).
- [18] Y. Hao, L. Inhester, K. Hanasaki, S.-K. Son, and R. Santra, Efficient electronic structure calculation for molecular ionization dynamics at high x-ray intensity, *Struct. Dyn.* **2**, 041707 (2015).
- [19] L. Inhester, K. Hanasaki, Y. Hao, S.-K. Son, and R. Santra, X-ray multiphoton ionization dynamics of a water molecule irradiated by an x-ray free-electron laser pulse, *Phys. Rev. A* **94**, 023422 (2016).
- [20] B. Rudek, K. Toyota, L. Foucar, B. Erk, R. Boll, C. Bomme, J. Correa, S. Carron, S. Boutet, G. J. Williams, K. R. Ferguson, R. Alonso-Mori, J. E. Koglin, T. Gorkhover, M. Bucher, C. S. Lehmann, B. Krässig, S. H. Southworth, L. Young, C. Bostedt *et al.*, Relativistic and resonant effects in the ionization of heavy atoms by ultra-intense hard X-rays, *Nat. Commun.* **9**, 4200 (2018).
- [21] R. Guichard, M. Richter, J.-M. Rost, U. Saalman, A. A. Sorokin, and K. Tiedtke, Multiple ionization of neon by soft x-rays at ultrahigh intensity, *J. Phys. B: At., Mol. Opt. Phys.* **46**, 164025 (2013).
- [22] M. Richter, A. A. Sorokin, and K. Tiedtke, The impact of pulse duration on multiphoton ionization in the soft X-ray regime, *Proc. SPIE* **8778**, 877808 (2013).
- [23] N. Gerken, S. Klumpp, A. A. Sorokin, K. Tiedtke, M. Richter, V. Bürk, K. Mertens, P. Juranić, and M. Martins, Time-Dependent Multiphoton Ionization of Xenon in the Soft-X-Ray Regime, *Phys. Rev. Lett.* **112**, 213002 (2014).
- [24] X. Li, L. Inhester, S. J. Robatjazi, B. Erk, R. Boll, K. Hanasaki, K. Toyota, Y. Hao, C. Bomme, B. Rudek, L. Foucar, S. H. Southworth, C. S. Lehmann, B. Kraessig, T. Marchenko, M. Simon, K. Ueda, K. R. Ferguson, M. Bucher, T. Gorkhover *et al.*, Pulse Energy and Pulse Duration Effects in the Ionization and Fragmentation of Iodomethane by Ultraintense Hard X Rays, *Phys. Rev. Lett.* **127**, 093202 (2021).
- [25] X. Li, L. Inhester, T. Osipov, R. Boll, R. Coffee, J. Cryan, A. Gattton, T. Gorkhover, G. Hartman, M. Ilchen, A. Knie, M.-F. Lin, M. P. Minitti, C. Weninger, T. J. A. Wolf, S.-K. Son, R. Santra, D. Rolles, A. Rudenko, and P. Walter, Electron-ion coincidence measurements of molecular dynamics with intense X-ray pulses, *Sci. Rep.* **11**, 505 (2021).
- [26] X. Li, Molecular response to ultra-intense x-rays studied with ion and electron momentum imaging, Ph.D. thesis, Kansas State University, 2019, Sec. 6.3.
- [27] R. D. Cowan, Atomic Structure Codes, <https://www.tcd.ie/Physics/people/Cormac.McGuinness/Cowan/>.
- [28] R. D. Cowan, *The Theory of Atomic Structure and Spectra* (University of California Press, Berkeley, CA, 1981).
- [29] M. Berger *et al.*, XCOM: Photon Cross Sections Database, 1998, <https://www.nist.gov/pml/xcom-photon-cross-sections-database>.
- [30] X. Li, A. Rudenko, M. S. Schöffler, N. Anders, T. M. Baumann, S. Eckart, B. Erk, A. De Fanis, K. Fehre, R. Dörner, L. Foucar, S. Grundmann, P. Grychtol, A. Hartung, M. Hofmann, M. Ilchen, C. Janke, G. Kastirke, M. Kircher, K. Kubicek *et al.*, Coulomb explosion imaging of small polyatomic molecules with ultrashort x-ray pulses (unpublished).
- [31] <https://doi.org/10.22003/xfel.eu-data-002159-00>.